Supporting Information

Intriguing Indium-salen Complexes as Multicolor Luminophores

Seon Hee Lee,[†,⊥] Nara Shin,[‡,⊥] Sang Woo Kwak,[§] Kyunglim Hyun,[§] Won Hee Woo,[§] Ji Hye Lee,[‡] Hyonseok Hwang,[‡] Min Kim,[§] Junseong Lee,[∥] Youngjo Kim,*[,§] Kang Mun Lee,*[,‡] and Myung Hwan Park*[,†]

[†]*Department of Chemistry Education, Chungbuk National University, Cheongju, Chungbuk 28644, Republic of Korea*

[‡]*Department of Chemistry and Institute for Molecular Science and Fusion Technology, Kangwon National University, Chuncheon, Gangwon 24341, Republic of Korea*

[§]*Department of Chemistry, Chungbuk National University, Cheongju, Chungbuk 28644, Republic of Korea*

[∥]*Department of Chemistry, Chonnam National University, Gwangju 61186, Republic of Korea*

Contents

^{1}H and ^{13}C NMR Spectra ····· S2
Crystallographic data and parameters for compound **3**, **4**, and **5** ····· S10
Selected bond lengths (Å) and angles (^{o}) for **3**, **4**, and **5** ····· S11
UV/Vis absorption and PL spectra in cyclohexane for **1**–**7** ····· S12
UV/Vis absorption and PL spectra in DMSO for **1**–**7** ····· S12
PL spectra in solid state for **1**–**7** ····· S12
Emission decay curve of **1**–**7** in THF solution ····· S13
Cyclic voltammograms of **1**–**7** ····· S14
Details of selected frontier orbitals of **1**–**7** at S_0 or S_1 state ····· S15
Frontier molecular orbitals for **1**–**7** at their ground state (S_0) ····· S29
^{1}H and ^{13}C NMR Spectra for $InMe_3$ ····· S30

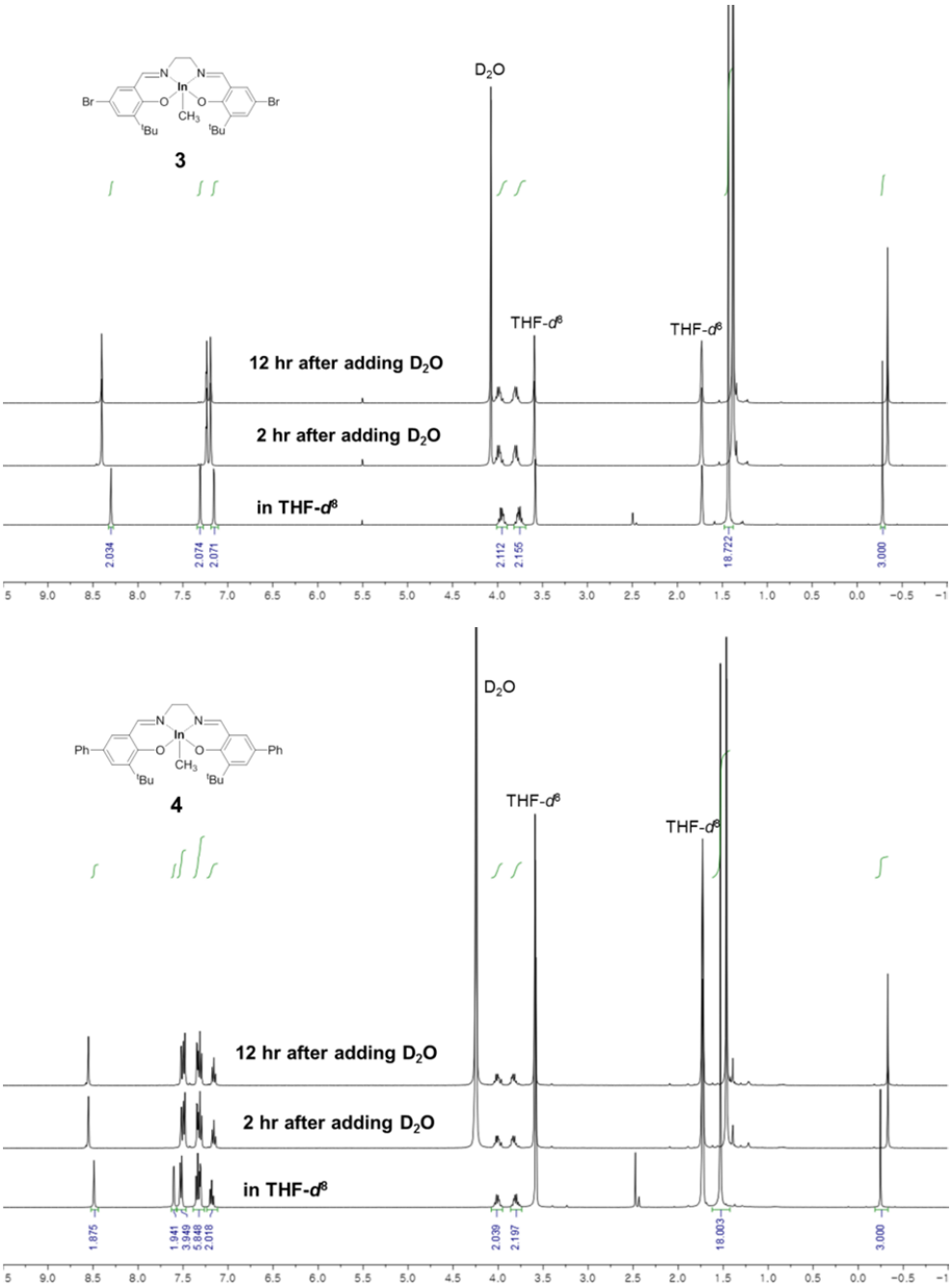

Figure S1. ^{1}H NMR spectra of **3** (top) and **4** (bottom) in THF-d^{8} and THF-d^{8}/D_2O (v/v = 4/1)

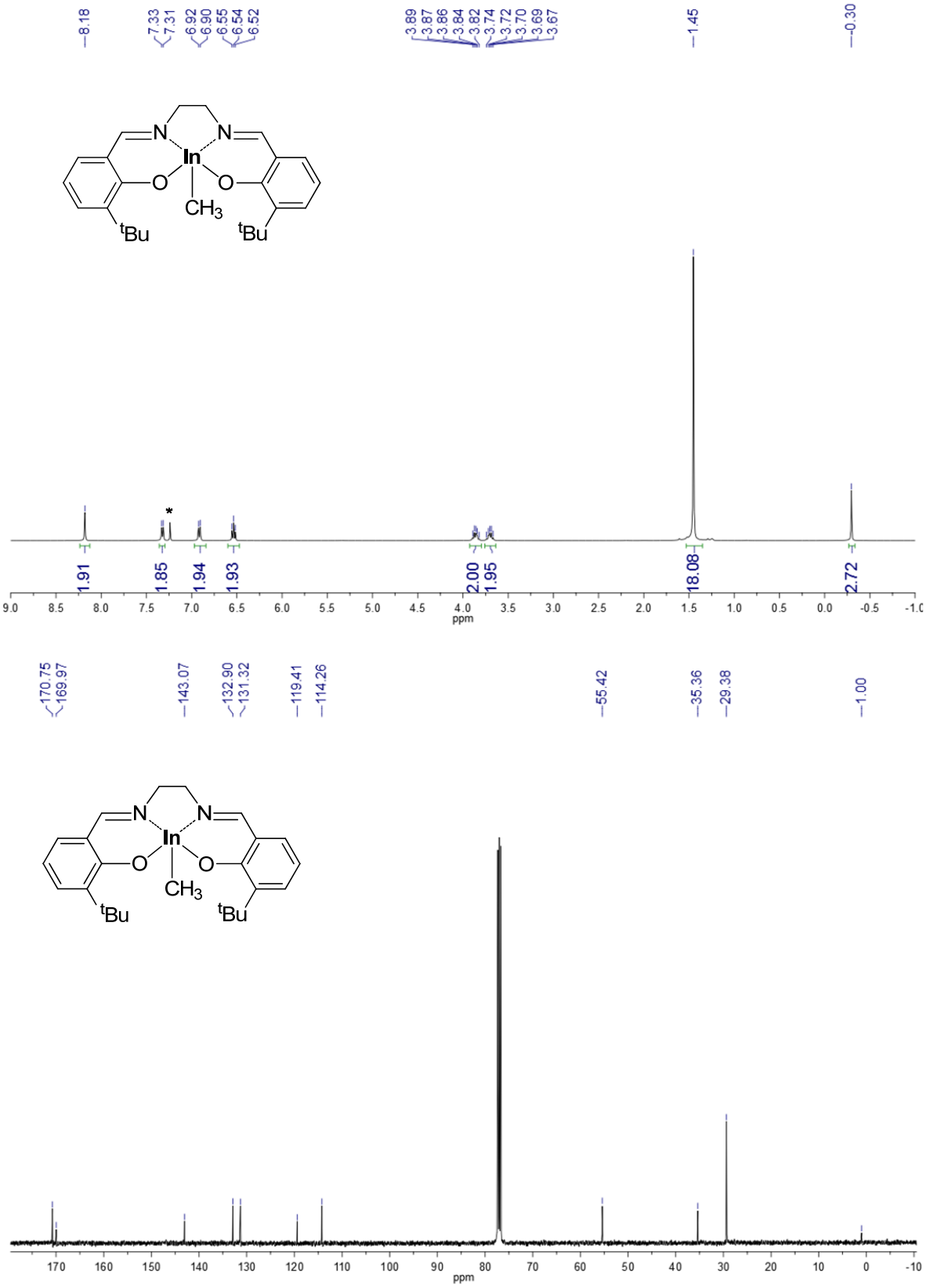

Figure S2. ^{1}H NMR (top) and ^{13}C (bottom) NMR spectra of **1** (∗ from residual $CHCl_3$ in $CDCl_3$).

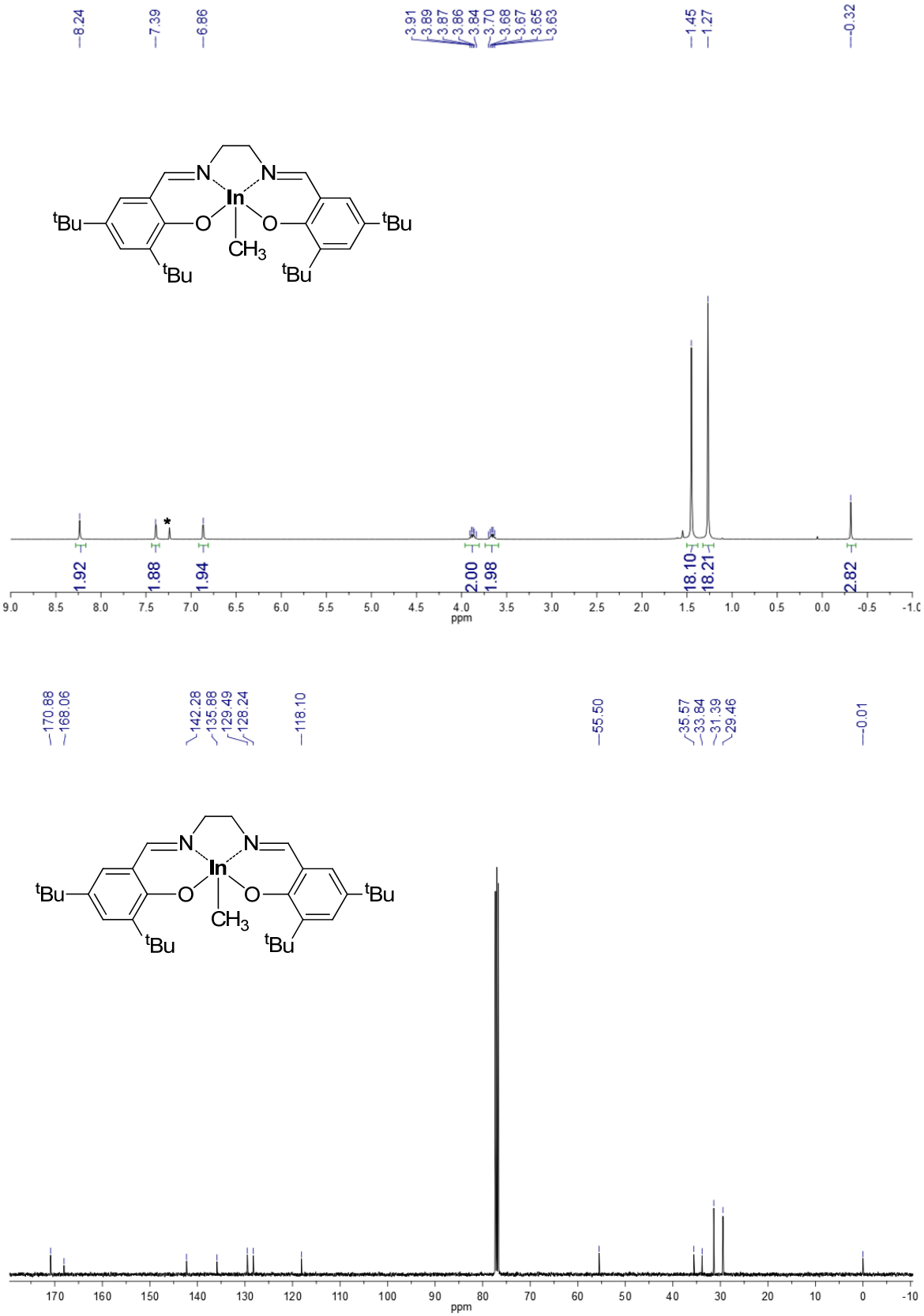

Figure S3. ^{1}H NMR (top) and ^{13}C (bottom) NMR spectra of **2** (∗ from residual $CHCl_3$ in $CDCl_3$).

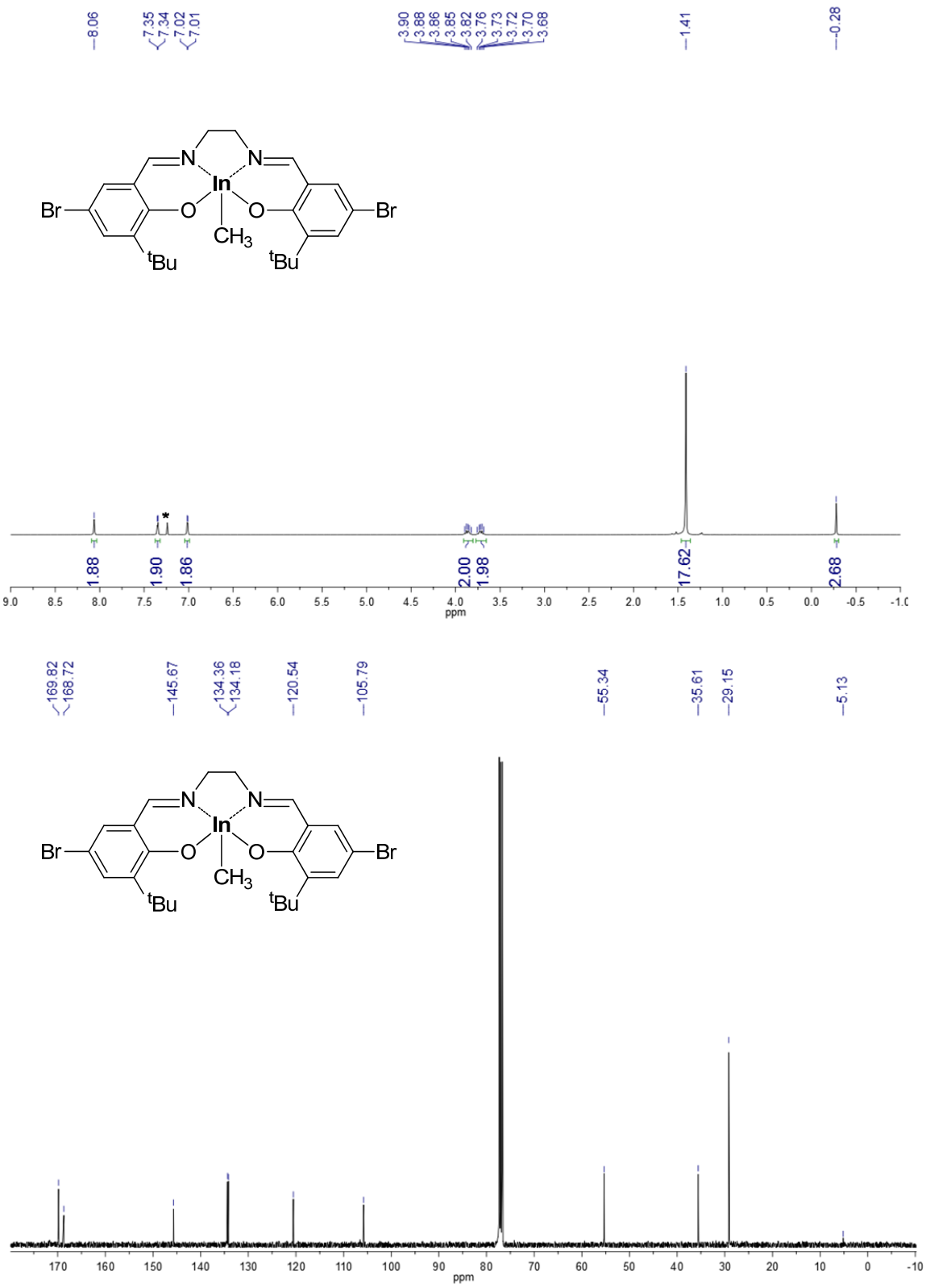

Figure S4. ^{1}H NMR (top) and ^{13}C (bottom) NMR spectra of **3** (∗ from residual $CHCl_3$ in $CDCl_3$).

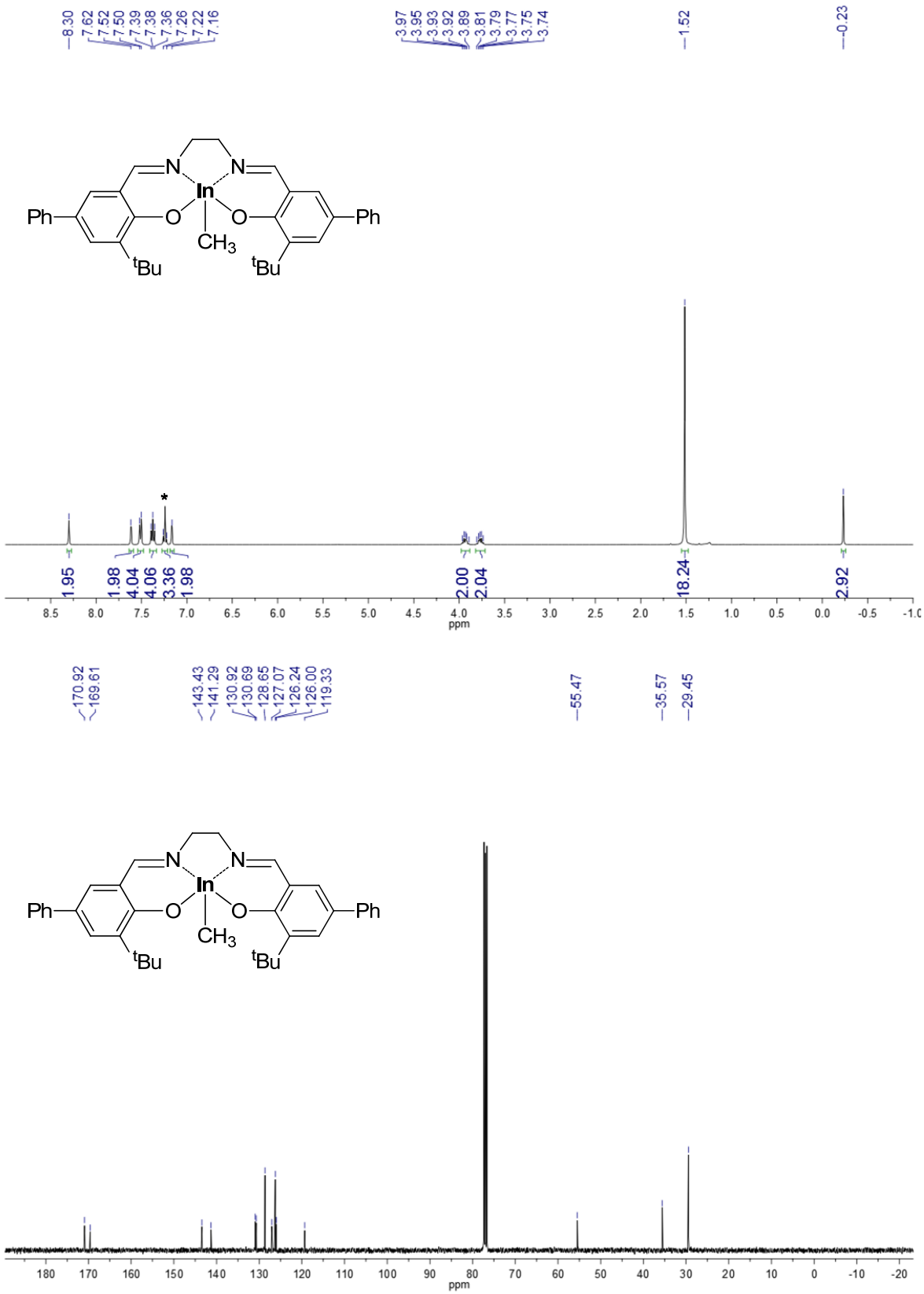

Figure S5. ^{1}H NMR (top) and ^{13}C (bottom) NMR spectra of **4** (∗ from residual $CHCl_3$ in $CDCl_3$).

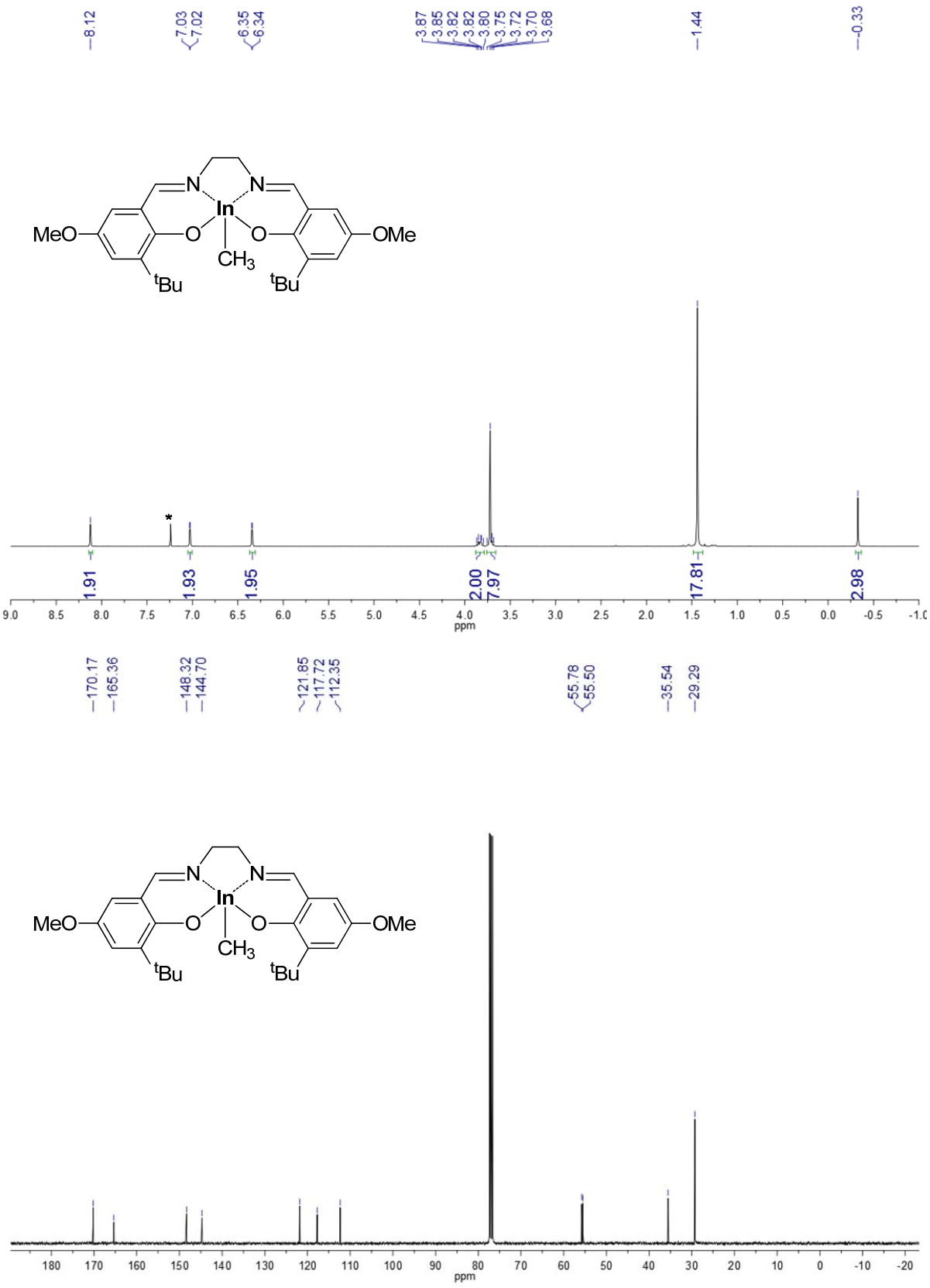

Figure S6. ^{1}H NMR (top) and ^{13}C (bottom) NMR spectra of **5** (∗ from residual $CHCl_3$ in $CDCl_3$).

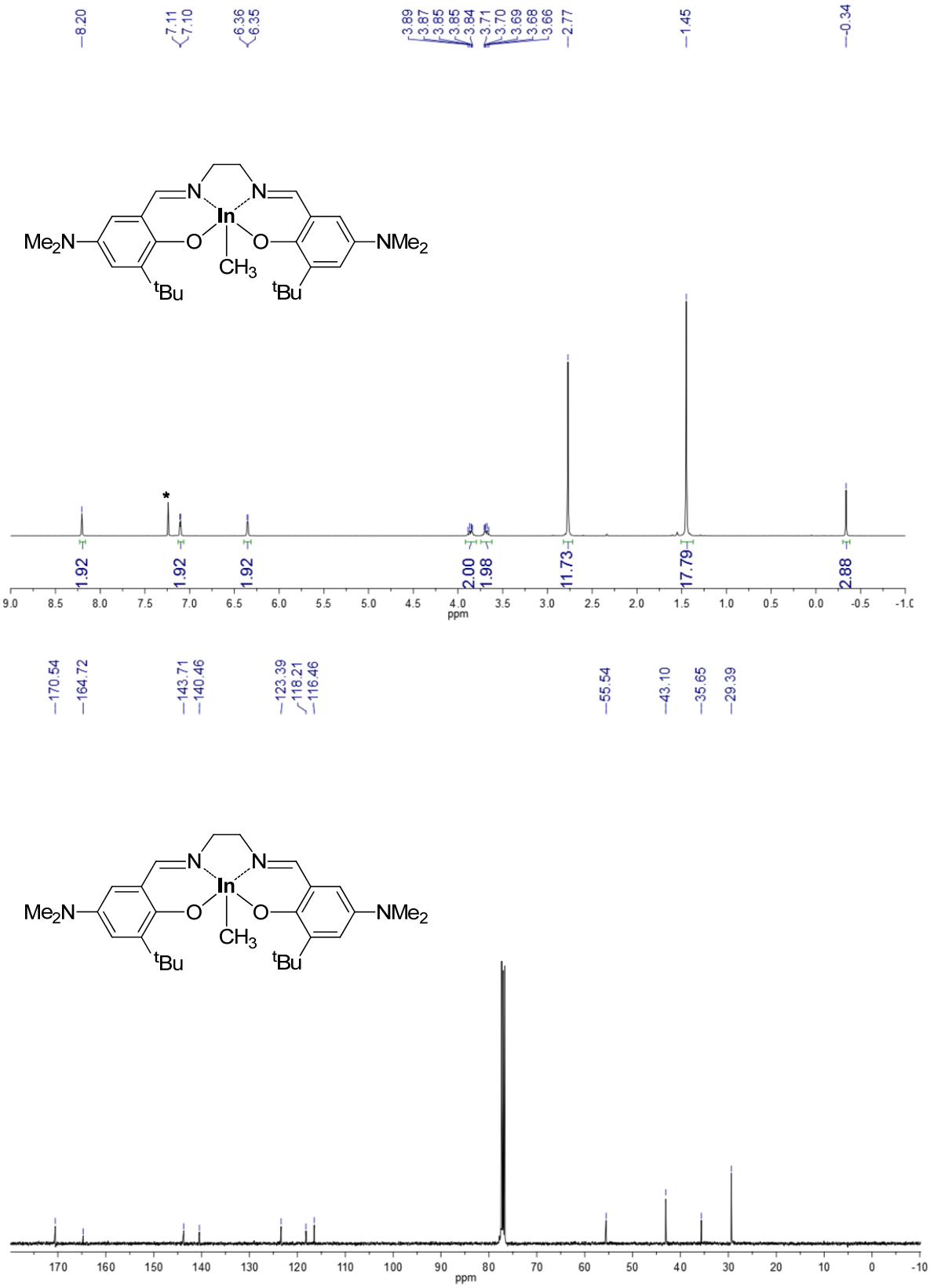

Figure S7. ^{1}H NMR (top) and ^{13}C (bottom) NMR spectra of **6** (∗ from residual $CHCl_3$ in $CDCl_3$).

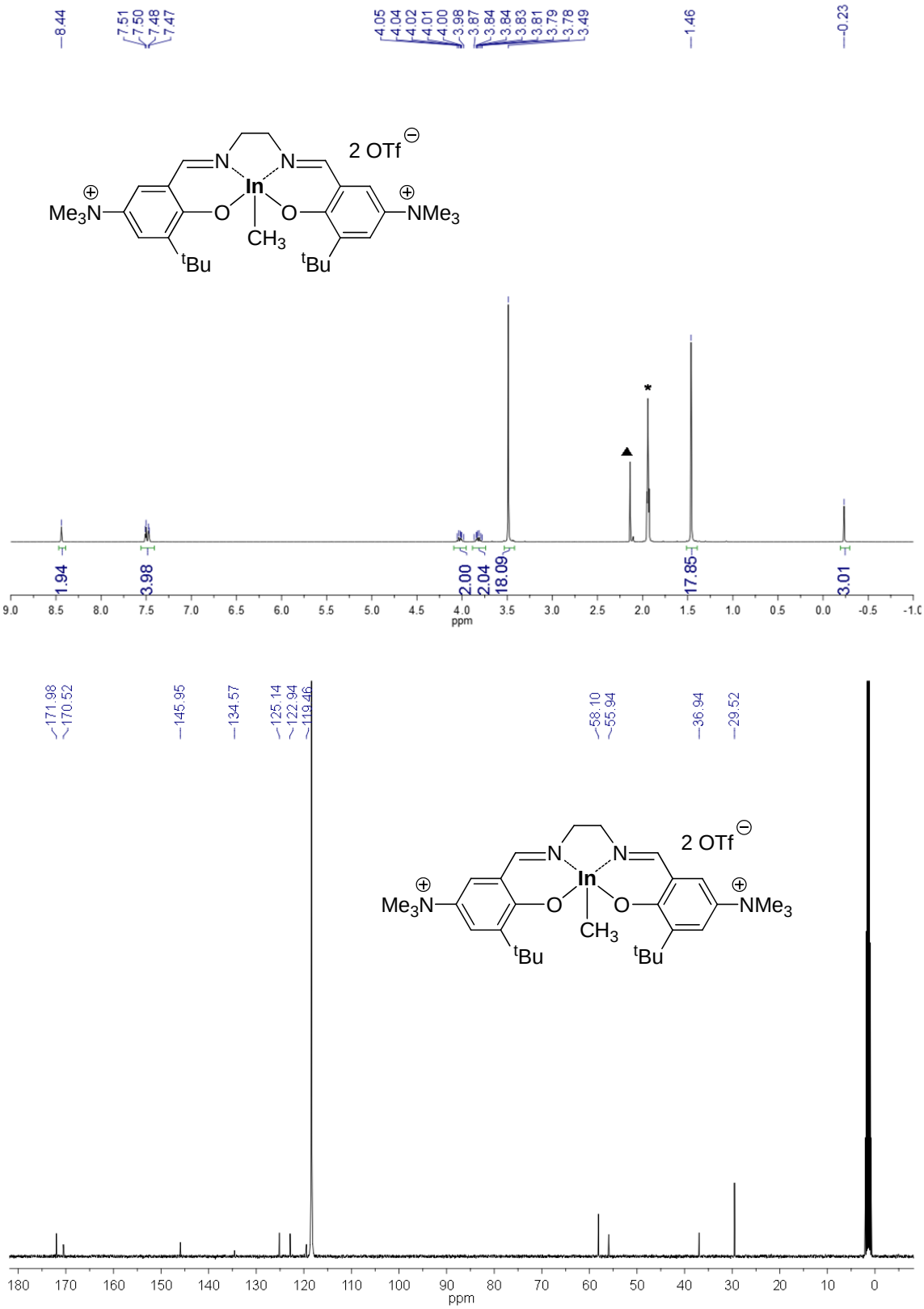

Figure S8. ^{1}H NMR (top) and ^{13}C (bottom) NMR spectra of **7** (∗from residual CH_3CN and ▲ from residual H_2O in CD_3CN).

Table S1. Crystallographic data and parameters for compound **3**, **4**, and **5**

Compound	**3**	(**4**·O(C_2H_5)$_2$)$_2$	**5**
Formula	$C_{25}H_{31}Br_2In_1N_2O_2$	$C_{78}H_{86}In_2N_4O_5$	$C_{27}H_{37}In_1N_2O_4$
Fomula weight	666.16	1389.14	568.40
Crystal system	Trigonal	Monoclinic	Orthorhombic
Space group	*R*–3	*P*2$_1$/*n*	*Pbca*
a (Å)	40.4131(5)	15.8881(10)	8.7418(13)
b (Å)	40.4131(5)	28.3612(17)	24.418(4)
c (Å)	9.8061(2)	18.5279(12)	25.523(4)
α (°)	90	90	90
β (°)	90	107.547(4)	90
γ (°)	120	90	90
V (Å^3)	13869.8(5)	7960.3(9)	5448.1(15)
Z	18	4	8
ρ_{calc}(g cm^{-3})	1.436	1.159	1.386
μ (mm^{-1})	3.380	0.626	0.901
F(000)	5940	2880	2352
T (K)	100	296	100
Scan mode	*multi*	*multi*	*multi*
hkl range	–45 → +45, –48 → +48, –11 → +11	–18 → +19, –34 → +34, –22 → +22	–10 → +10, –29 → +29, –30 → +30
Measd reflns	30805	66682	63588
Unique reflns [R_{int}]	5666 [0.0736]	9726 [0.1087]	4979 [0.0573]
Reflns used for refinement	5666	9726	4979
Refined parameters	296	863	316
R_1 [a] (I>2σ(I))	0.0402	0.0811	0.0444
wR_2[b] all data	0.1016	0.2434	0.1163
GOF on F^2	1.014	1.024	1.021
ρ_{fin} (max/min) (e Å^{-3})	0.909, –1.602	1.106, –1.677	1.142, –0.737

[a] $R_1 = \sum||Fo| - |Fc||/\sum|Fo|$. [b] $wR_2 = \{[\sum w(Fo^2 - Fc^2)^2]/[\sum w(Fo^2)^2]\}^{1/2}$.

Table S2. Selected bond lengths (Å) and angles (^{o}) for **3**, **4**, and **5**

Compound	**3**	**4**	**5**
		lengths	
In–N1	2.242(3)	2.242(6)	2.250(4)
In–N2	2.236(3)	2.239(6)	2.255(4)
In–O1	2.102(3)	2.105(5)	2.084(3)
In–O2	2.100(2)	2.067(5)	2.093(3)
In–C25	2.129(4)	–	–
In–C27	–	–	2.134(6)
In–C37	–	2.142(8)	
		Angles	
N1–In–N2	72.87(11)	73.7(2)	72.15(15
N1–In–O1	81.23(11)	81.40(2)	81.39(13)
O1–In–O2	88.65(9)	85.40(19)	88.25(12)
N2–In–O2	81.00(10)	81.90(2)	78.94(13)
N1–In–O2	120.20(11)	126.1(2)	126.62(14)
N2–In–O1	141.80(12)	137.0(2)	134.04(14)
N1–In–C25	125.30(14)	–	–
N2–In–C25	107.21(17)	–	–
O1–In–C25	110.63(16)	–	–
O2–In–C25	113.47(14)	–	–
N1–In–C27	–	–	115.6(2)
N2–In–C27	–	–	112.1(2)
O1–In–C27	–	–	113.1(2)
O2–In–C27	–	–	116.7(2)
N1–In–C37	–	113.3(3)	–
N2–In–C37	–	109.1(3)	–
O1–In–C37	–	112.8(3)	–
O2–In–C37	–	120.0(3)	–

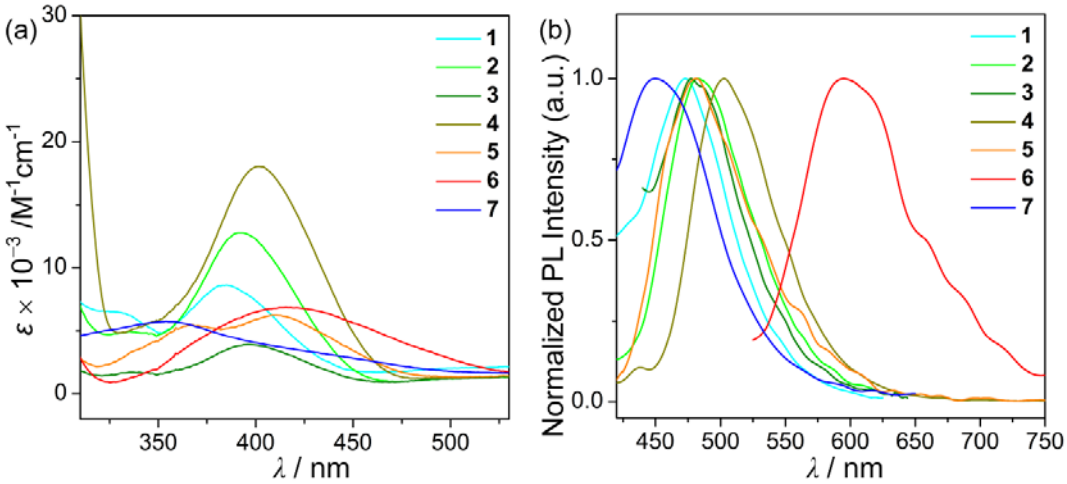

Figure S9. (a) UV/Vis absorption and (b) PL spectra in cyclohexane (1.0×10^{-5} M) for **1**–**7**.

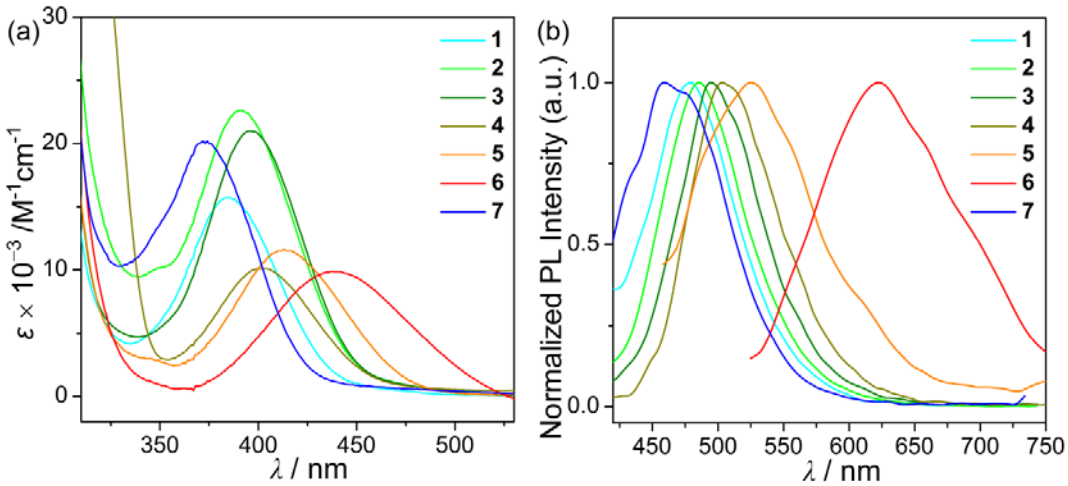

Figure S10. (a) UV/Vis absorption and (b) PL spectra in DMSO (1.0×10^{-5} M) for **1**–**7**.

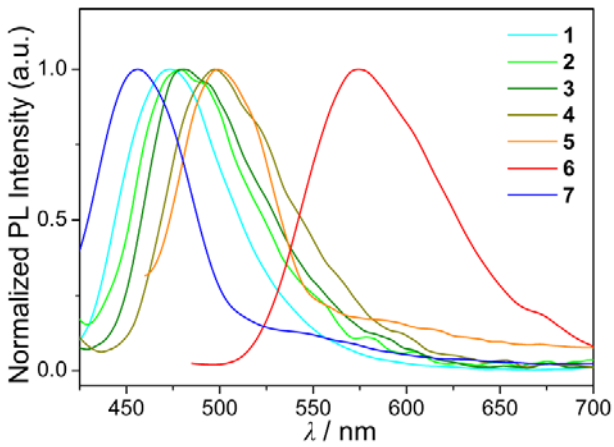

Figure S11. PL spectra in solid state for **1**–**7**.

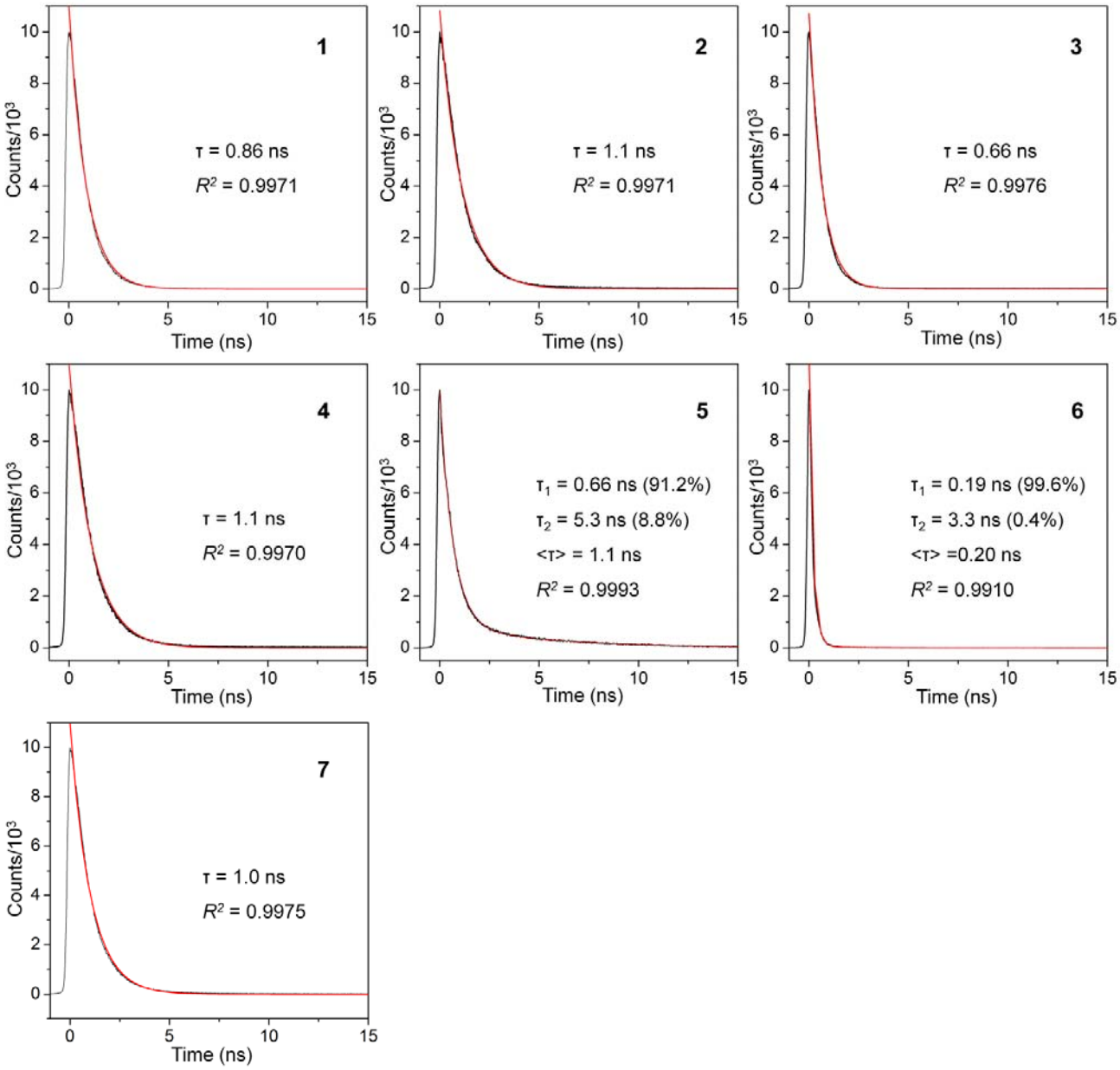

Figure S12. Emission decay curves of **1**–**7** in THF solution (1.0×10^{-5} M) at 298 K and their exponential fitting curves (red-line, single or double exponential curve fitting).

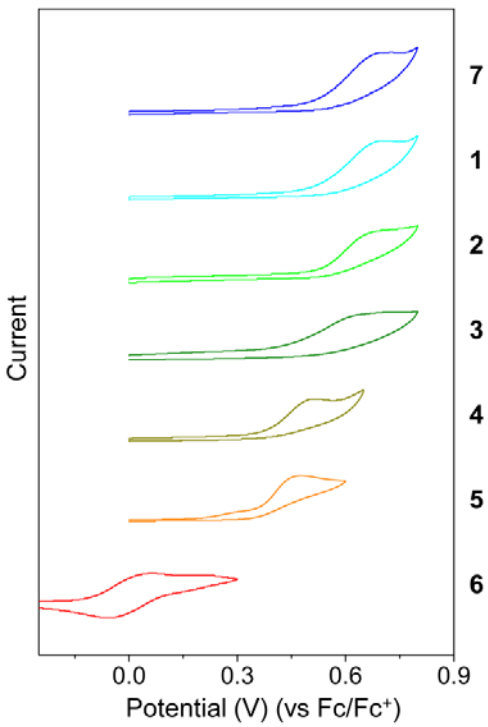

Figure S13. Cyclic voltammograms (CV) of **1**–**7** showing oxidation (5×10^{-4} M in DMSO, scan rate = 100 mV/s for oxidation).

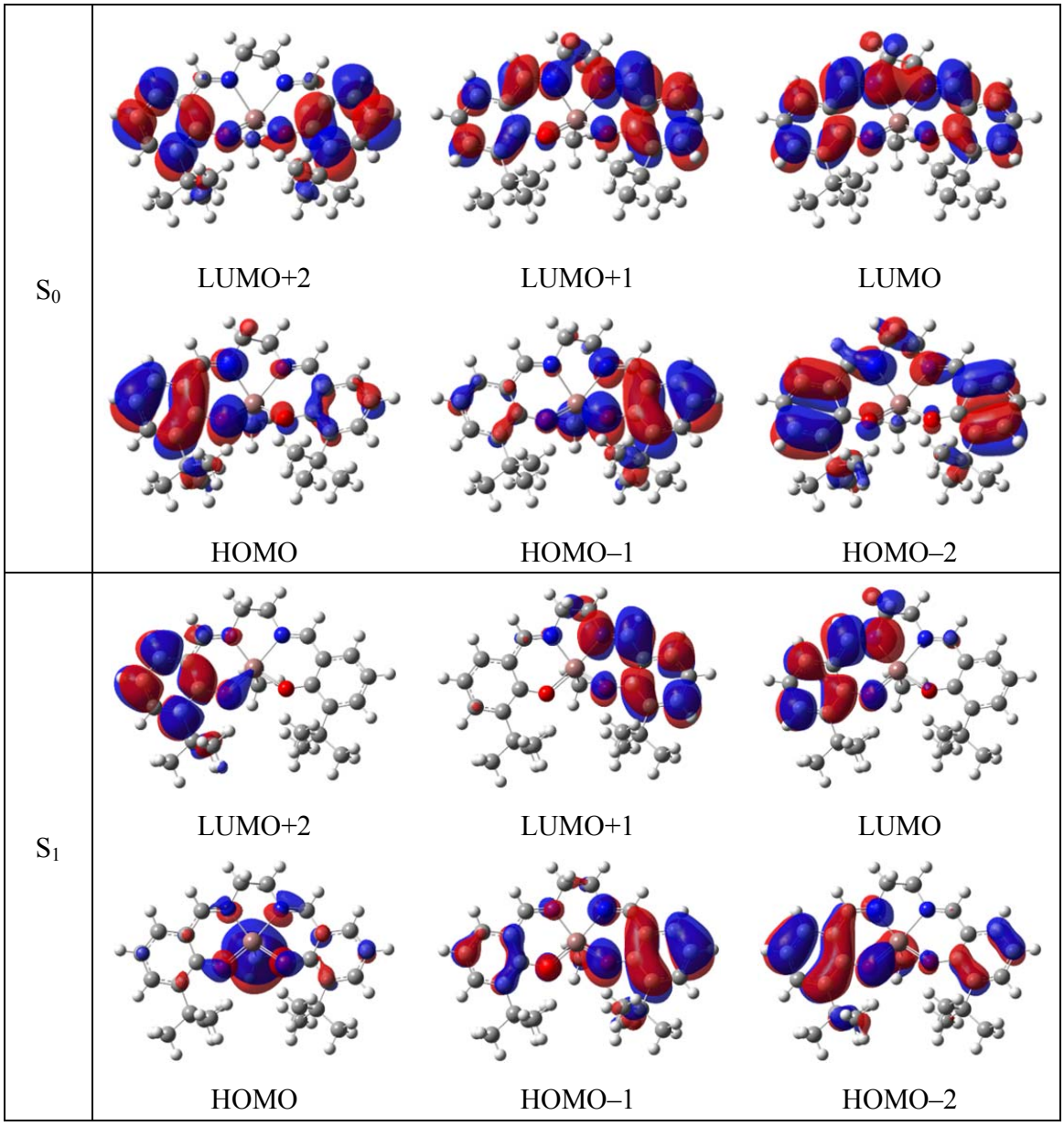

Figure S14. The selected frontier orbitals of **1** from B3LYP calculations (Isovalue = 0.04 a.u.) at the ground state (S_0) and first singlet excited state (S_1) optimized geometries in toluene.

Table S3. Computed absorption wavelengths (λ_{calc} in nm) and oscillator strengths ($f_{calc.}$) for **1** from TD-B3LYP calculations using the B3LYP geometries at the ground state (S_0) and first singlet excited state (S_1) optimized geometries in toluene

state	λ_{calc} (/nm)	f_{calc}	Major contribution
			S_0
1	375.38	0.0398	HOMO → LUMO (95.4%)
2	366.47	0.0825	HOMO−1 → LUMO (96.6%)
3	339.58	0.0011	HOMO−1 → LUMO+1 (47.8%)
			HOMO → LUMO+1 (48.7%)
			S_1
1	991.73	0.0014	HOMO → LUMO (99.8%)
2	610.28	0.0027	HOMO → LUMO+1 (99.7%)
3	438.73	0.0154	HOMO−1 → LUMO (99.1%)

Table S4. Molecular orbital energies (in eV) and molecular orbital distributions (in %) of **1** at the ground state (S_0) and first singlet excited state (S_1) optimized geometries in toluene

	E (eV)	Imine bridge	Phenyl rings	In–CH_3
		S_0		
LUMO+2	0.30	1.7	96.8	1.5
LUMO+1	−1.34	52.5	47.4	0.1
LUMO	−1.63	56.2	42.7	1.1
HOMO	−5.49	7.3	90.4	2.3
HOMO−1	−5.54	5.9	89.6	4.5
HOMO−2	−6.54	18.8	80.6	0.6
		S_1		
LUMO+2	0.07	2.0	96.4	1.7
LUMO+1	−1.44	53.8	45.6	0.5
LUMO	−2.28	55.7	43.7	0.6
HOMO	−4.21	4.0	12.0	84.0
HOMO−1	−5.60	6.6	90.8	2.6
HOMO−2	−6.05	4.3	89.2	6.4

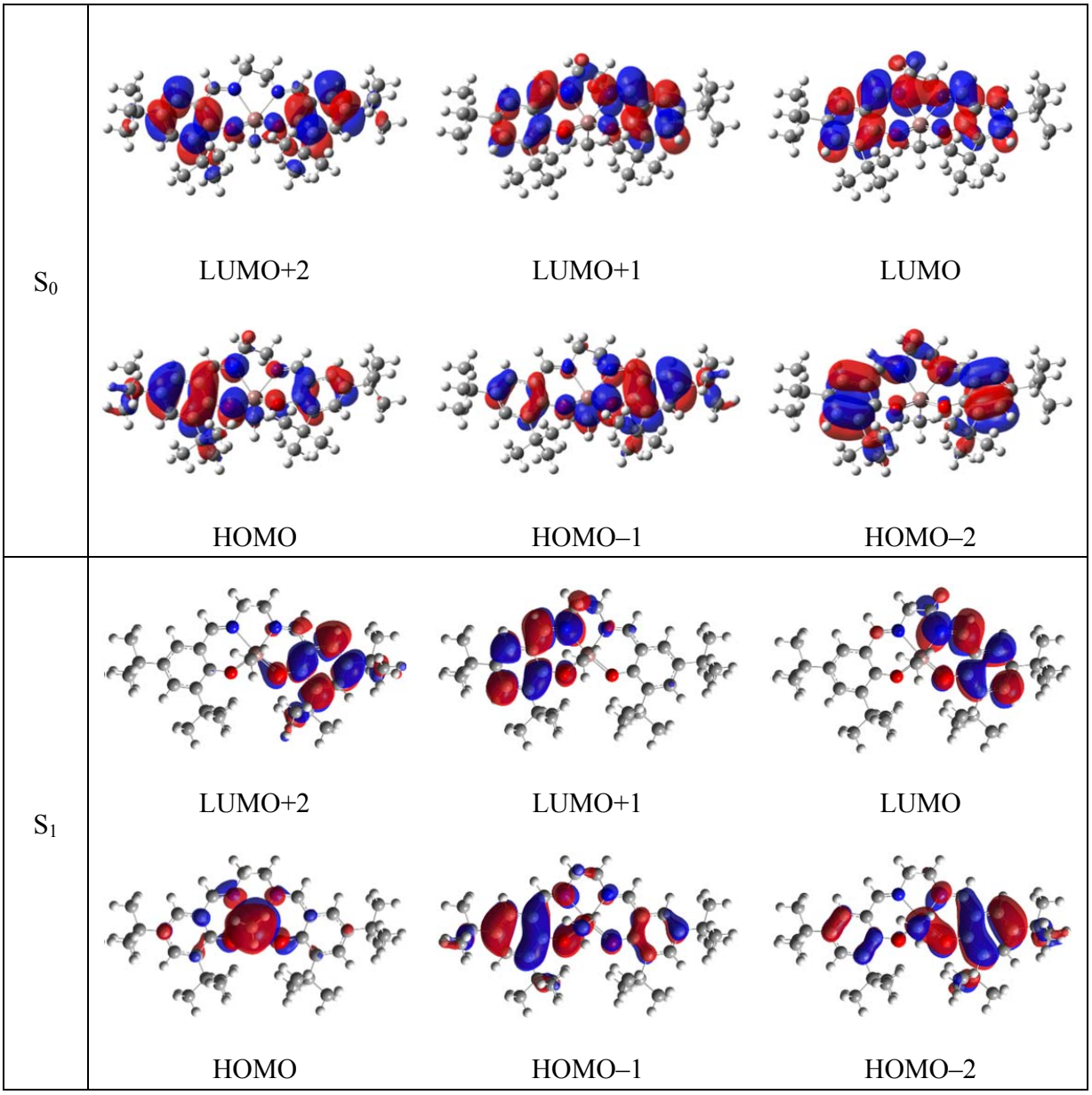

Figure S15. The selected frontier orbitals of **2** from B3LYP calculations (Isovalue = 0.04 a.u.) at the ground state (S_0) and first singlet excited state (S_1) optimized geometries in toluene.

Table S5. Computed absorption wavelengths (λ_{calc} in nm) and oscillator strengths ($f_{calc.}$) for **2** from TD-B3LYP calculations using the B3LYP geometries at the ground state (S_0) and first singlet excited state (S_1) optimized geometries in toluene

state	λ_{calc} (/nm)	f_{calc}	Major contribution
			S_0
1	383.44	0.0357	HOMO → LUMO (96.5%)
2	374.15	0.0832	HOMO−1 → LUMO (97.9%)
3	346.23	0.0040	HOMO−1 → LUMO+1 (49.3%)
			HOMO → LUMO+1 (48.0%)
			S_1
1	972.20	0.0015	HOMO → LUMO (99.8%)
2	604.19	0.0030	HOMO → LUMO+1 (99.7%)
3	451.33	0.0180	HOMO−1 → LUMO (99.3%)

Table S6. Molecular orbital energies (in eV) and molecular orbital distributions (in %) of **2** at the ground state (S_0) and first singlet excited state (S_1) optimized geometries in toluene

	E (eV)	Imine bridge	Phenyl rings	In–CH_3
		S_0		
LUMO+2	0.38	1.9	96.7	1.5
LUMO+1	−1.30	51.9	48.0	0.1
LUMO	−1.59	55.7	43.3	1.1
HOMO	−5.36	7.5	90.9	1.5
HOMO−1	−5.41	6.1	89.3	4.5
HOMO−2	−6.48	17.5	82.1	0.4
		S_1		
LUMO+2	0.15	2.1	96.2	1.7
LUMO+1	−1.39	53.3	46.1	0.5
LUMO	−2.23	55.3	44.2	0.6
HOMO	−4.18	4.1	12.7	83.2
HOMO−1	−5.46	6.8	90.1	3.1
HOMO−2	−5.92	5.0	88.3	6.7

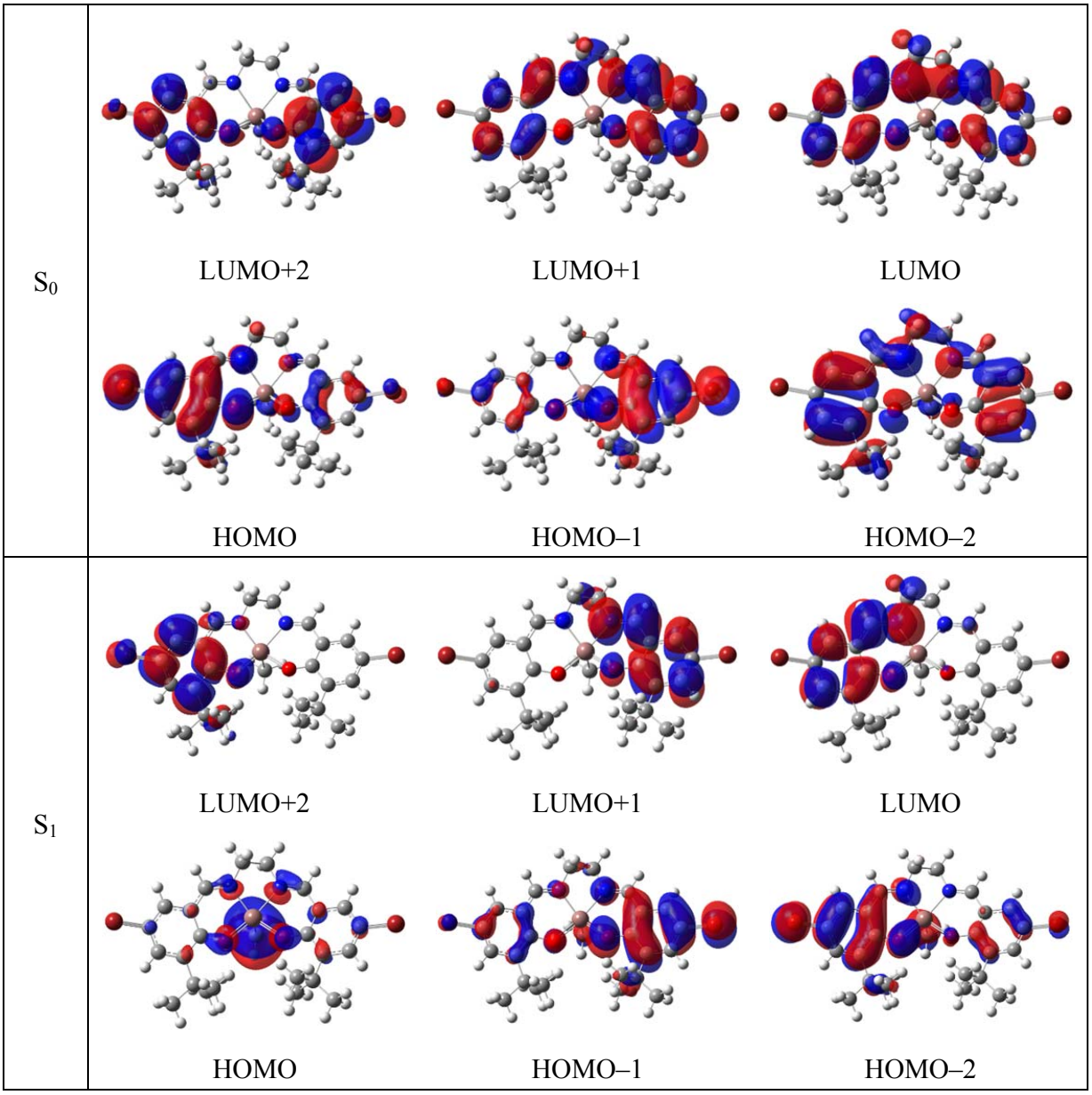

Figure S16. The selected frontier orbitals of **3** from B3LYP calculations (Isovalue = 0.04 a.u.) at the ground state (S_0) and first singlet excited state (S_1) optimized geometries in toluene.

Table S7. Computed absorption wavelengths (λ_{calc} in nm) and oscillator strengths ($f_{calc.}$) for **3** from TD-B3LYP calculations using the B3LYP geometries at the ground state (S_0) and first singlet excited state (S_1) optimized geometries in toluene

state	λ_{calc} (/nm)	f_{calc}	Major contribution
			S_0
1	385.37	0.0399	HOMO → LUMO (95.6%)
2	376.54	0.0845	HOMO−1 → LUMO (97.1%)
3	348.95	0.0007	HOMO−1 → LUMO+1 (57.3%)
			HOMO → LUMO+1 (39.1%)
			S_1
1	1054.54	0.0015	HOMO → LUMO (99.8%)
2	630.62	0.0025	HOMO → LUMO+1 (99.7%)
3	454.46	0.0174	HOMO−1 → LUMO (99.2%)

Table S8. Molecular orbital energies (in eV) and molecular orbital distributions (in %) of **3** at the ground state (S_0) and first singlet excited state (S_1) optimized geometries in toluene

	E (eV)	Imine bridge	Phenyl rings	In–CH_3
		S_0		
LUMO+2	−0.04	1.6	97.0	1.4
LUMO+1	−1.57	50.7	49.2	0.1
LUMO	−1.85	54.9	44.1	1.1
HOMO	−5.61	6.9	91.2	1.9
HOMO−1	−5.65	5.7	90.1	4.2
HOMO−2	−6.83	19.4	78.8	1.8
		S_1		
LUMO+2	−0.25	1.9	97.1	1.0
LUMO+1	−1.67	52.2	47.3	0.5
LUMO	−2.50	54.2	45.2	0.6
HOMO	−4.37	4.0	12.0	84.0
HOMO−1	−5.70	6.2	91.2	2.6
HOMO−2	−6.14	4.9	88.9	6.2

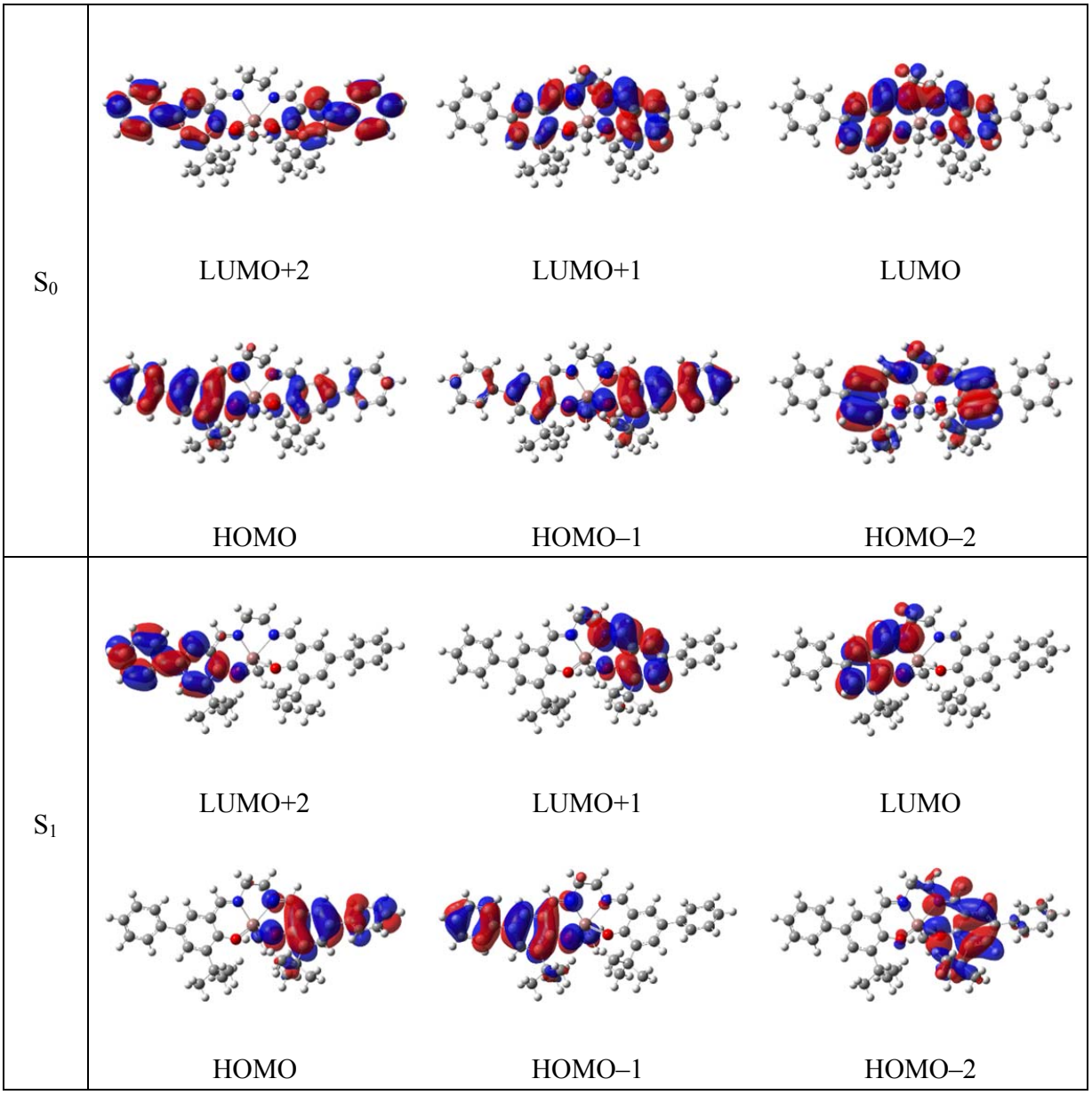

Figure S17. The selected frontier orbitals of **4** from B3LYP calculations (Isovalue = 0.04 a.u.) at the ground state (S_0) and first singlet excited state (S_1) optimized geometries in toluene.

Table S9. Computed absorption wavelengths (λ_{calc} in nm) and oscillator strengths ($f_{calc.}$) for **4** from TD-B3LYP calculations using the B3LYP geometries at the ground state (S_0) and first singlet excited state (S_1) optimized geometries in toluene

state	λ_{calc} (/nm)	f_{calc}	Major contribution
			S_0
1	398.07	0.0412	HOMO → LUMO (96.2%)
2	387.91	0.0773	HOMO−1 → LUMO (97.4%)
3	357.61	0.0521	HOMO−1 → LUMO+1 (88.0%)
			S_1
1	611.35	0.0023	HOMO → LUMO (99.7%)
2	463.85	0.0685	HOMO−1 → LUMO (97.8%)

Table S10. Molecular orbital energies (in eV) and molecular orbital distributions (in %) of **4** at the ground state (S_0) and first singlet excited state (S_1) optimized geometries in toluene

	E (eV)	Imine bridge	Phenyl rings	In–CH_3
		S_0		
LUMO+2	−0.55	0.4	98.9	0.7
LUMO+1	−1.41	52.0	47.9	0.1
LUMO	−1.70	56.0	43.0	1.1
HOMO	−5.33	5.8	93.1	1.1
HOMO−1	−5.38	4.8	91.7	3.4
HOMO−2	−6.62	16.8	82.4	0.7
		S_1		
LUMO+2	−0.72	0.4	99.2	0.4
LUMO+1	−1.11	54.7	45.0	0.3
LUMO	−2.35	55.7	43.3	1.1
HOMO	−4.82	5.0	93.9	1.1
HOMO−1	−5.66	6.3	90.3	3.3
HOMO−2	−6.46	14.1	85.6	0.3

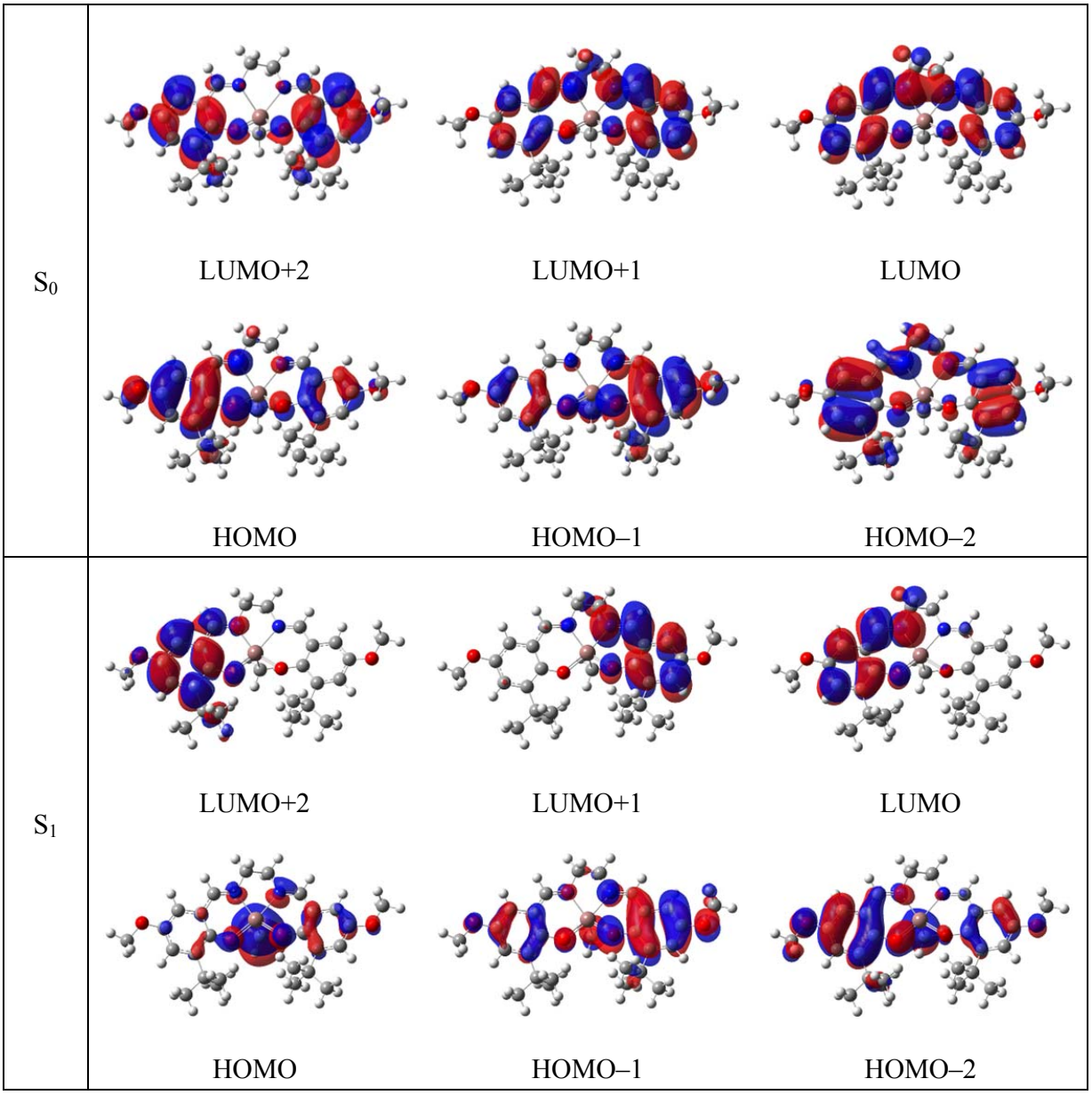

Figure S18. The selected frontier orbitals of **5** from B3LYP calculations (Isovalue = 0.04 a.u.) at the ground state (S_0) and first singlet excited state (S_1) optimized geometries in toluene.

Table S11. Computed absorption wavelengths (λ_{calc} in nm) and oscillator strengths ($f_{calc.}$) for **5** from TD-B3LYP calculations using the B3LYP geometries at the ground state (S_0) and first singlet excited state (S_1) optimized geometries in toluene

state	λ_{calc} (/nm)	f_{calc}	Major contribution
			S_0
1	393.43	0.0326	HOMO → LUMO (96.4%)
2	384.07	0.0895	HOMO−1 → LUMO (97.8%)
3	355.37	0.0062	HOMO−1 → LUMO+1 (46.7%)
			HOMO → LUMO+1 (50.9%)
			S_1
1	919.35	0.0025	HOMO → LUMO (99.5%)
2	575.78	0.0051	HOMO → LUMO+1 (99.4%)
3	513.97	0.0170	HOMO−1 → LUMO (99.4%)

Table S12. Molecular orbital energies (in eV) and molecular orbital distributions (in %) of **5** at the ground state (S_0) and first singlet excited state (S_1) optimized geometries in toluene

	E (eV)	Imine bridge	Phenyl rings	In–CH_3
		S_0		
LUMO+2	0.29	3.3	95.3	1.3
LUMO+1	−1.40	51.4	48.5	0.1
LUMO	−1.68	55.3	43.6	1.1
HOMO	−5.37	7.2	91.3	1.5
HOMO−1	−5.41	5.9	89.8	4.3
HOMO−2	−6.61	18.0	81.2	0.8
		S_1		
LUMO+2	0.14	7.5	92.2	0.3
LUMO+1	−1.44	52.6	47.0	0.4
LUMO	−2.30	55.7	43.7	0.6
HOMO	−4.31	4.3	18.7	76.9
HOMO−1	−5.18	6.3	89.1	4.6
HOMO−2	−5.60	3.9	85.7	10.3

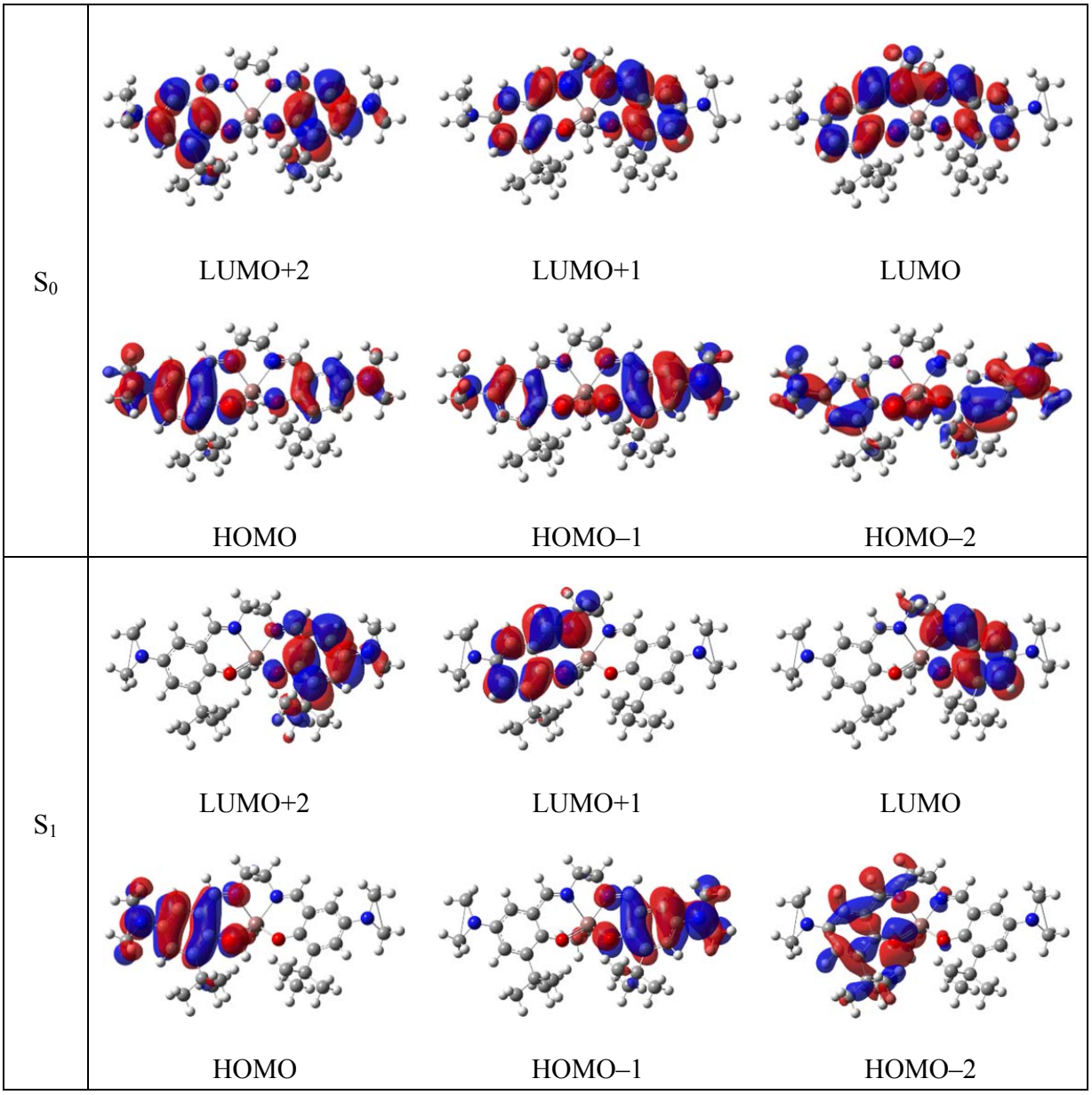

Figure S19. The selected frontier orbitals of **6** from B3LYP calculations (Isovalue = 0.04 a.u.) at the ground state (S_0) and first singlet excited state (S_1) optimized geometries in toluene.

Table S13. Computed absorption wavelengths (λ_{calc} in nm) and oscillator strengths ($f_{calc.}$) for **6** from TD-B3LYP calculations using the B3LYP geometries at the ground state (S_0) and first singlet excited state (S_1) optimized geometries in toluene

state	λ_{calc} (/nm)	f_{calc}	Major contribution
			S_0
1	447.85	0.0320	HOMO → LUMO (97.1%)
2	434.59	0.0787	HOMO−1 → LUMO (98.1%)
3	398.79	0.0611	HOMO−1 → LUMO+1 (33.8%)
			HOMO → LUMO+1 (63.5%)
			S_1
1	935.59	0.0032	HOMO → LUMO (99.8%)
2	530.41	0.0647	HOMO−1 → LUMO (10.3%)
			HOMO → LUMO+1 (89.4%)

Table S14. Molecular orbital energies (in eV) and molecular orbital distributions (in %) of **6** at the ground state (S_0) and first singlet excited state (S_1) optimized geometries in toluene

	E (eV)	Imine bridge	Phenyl rings	In–CH_3
		S_0		
LUMO+2	0.47	4.0	94.8	1.2
LUMO+1	−1.30	51.3	48.6	0.1
LUMO	−1.58	55.0	44.0	1.0
HOMO	−4.84	5.6	93.8	0.6
HOMO−1	−4.89	4.9	92.8	2.3
HOMO−2	−6.41	2.8	88.8	8.4
		S_1		
LUMO+2	0.23	4.4	95.2	0.3
LUMO+1	−1.00	55.9	42.9	1.1
LUMO	−2.18	53.4	46.0	0.5
HOMO	−3.92	5.5	93.4	1.1
HOMO−1	−5.26	5.7	93.0	1.3
HOMO−2	−6.11	12.8	84.4	2.8

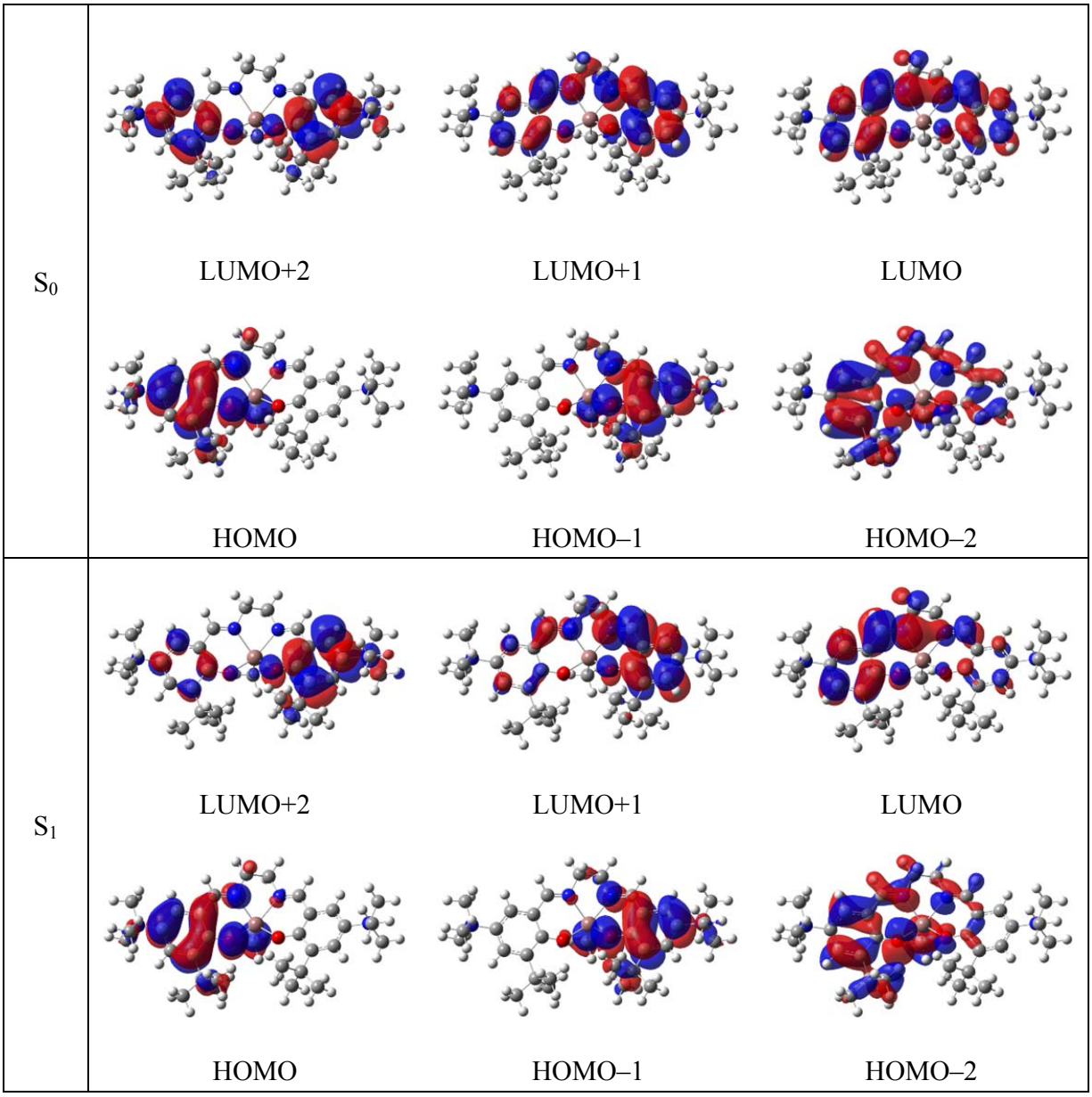

Figure S20. The selected frontier orbitals of **7** from B3LYP calculations (Isovalue = 0.04 a.u.) at the ground state (S_0) and first singlet excited state (S_1) optimized geometries in toluene.

Table S15. Computed absorption wavelengths (λ_{calc} in nm) and oscillator strengths ($f_{calc.}$) for **7** from TD-B3LYP calculations using the B3LYP geometries at the ground state (S_0) and first singlet excited state (S_1) optimized geometries in toluene

state	λ_{calc} (/nm)	f_{calc}	Major contribution
			S_0
1	359.55	0.0632	HOMO−1 → LUMO (3.7%)
			HOMO → LUMO (92.5%)
2	352.02	0.0712	HOMO−1 → LUMO (93.0%)
			HOMO → LUMO (4.2%)
			S_1
1	418.75	0.0882	HOMO → LUMO (98.0%)
2	380.12	0.0164	HOMO−1 → LUMO (98.5%)
3	357.84	0.0050	HOMO → LUMO+1 (97.3%)

Table S16. Molecular orbital energies (in eV) and molecular orbital distributions (in %) of **7** at the ground state (S_0) and first singlet excited state (S_1) optimized geometries in toluene

	E (eV)	Imine bridge	Phenyl rings	In–CH_3
		S_0		
LUMO+2	−0.98	0.5	98.3	1.3
LUMO+1	−2.34	47.5	52.4	0.1
LUMO	−2.61	52.5	46.5	1.0
HOMO	−6.61	8.6	85.3	6.2
HOMO−1	−6.66	7.5	88.6	3.9
HOMO−2	−7.64	21.3	74.0	4.7
		S_1		
LUMO+2	−0.98	0.6	98.5	0.9
LUMO+1	−2.46	49.4	50.5	0.1
LUMO	−2.89	56.7	42.1	1.3
HOMO	−6.42	6.9	87.1	6.0
HOMO−1	−6.68	7.4	87.6	5.1
HOMO−2	−7.59	15.2	72.5	12.2

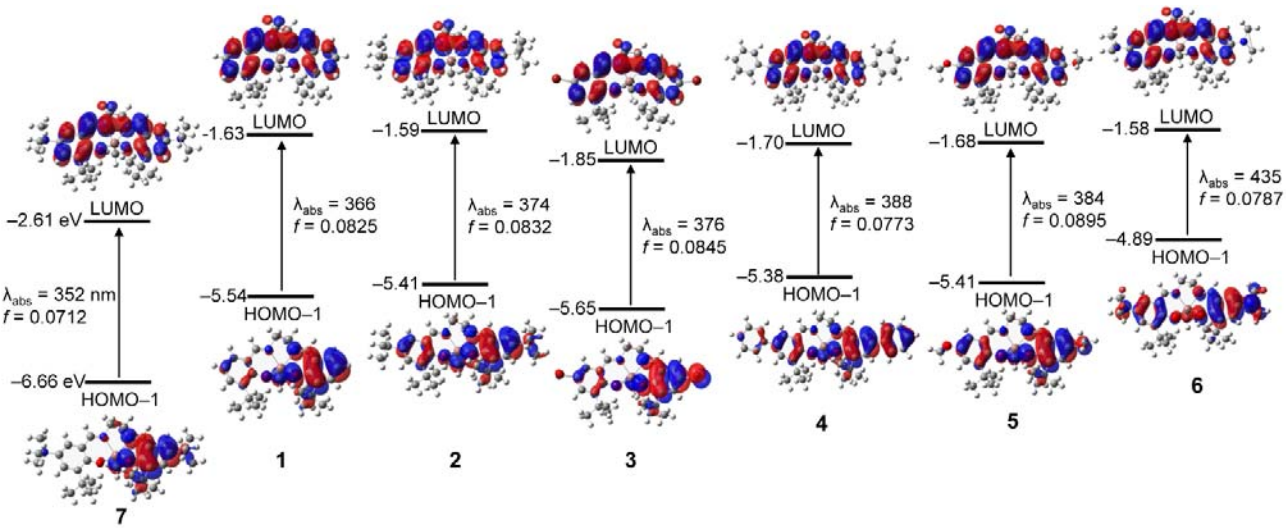

Figure S21. Frontier molecular orbitals for **1**–**7** at their ground state (S_0) with their relative energies from DFT calculation (isovalue = 0.04). The transition energy (in nm) was calculated using the TD-B3LYP method with 6-31G(d) basis sets.

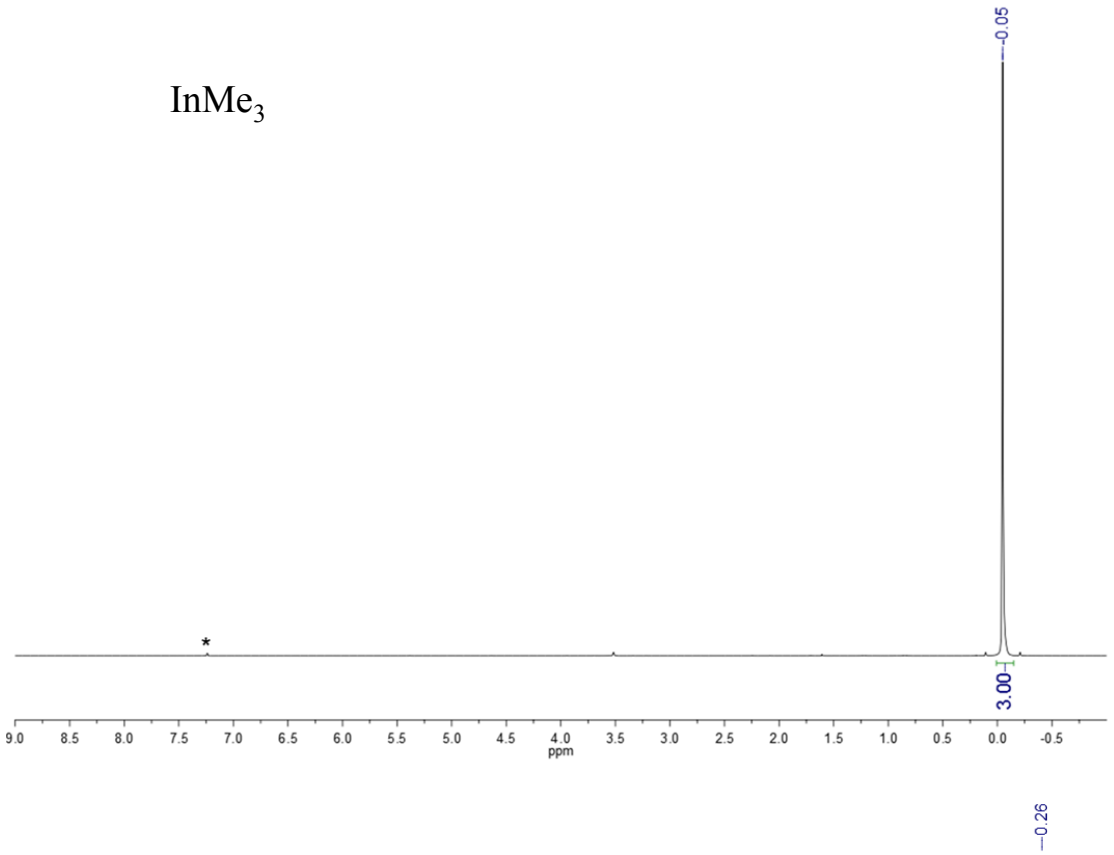

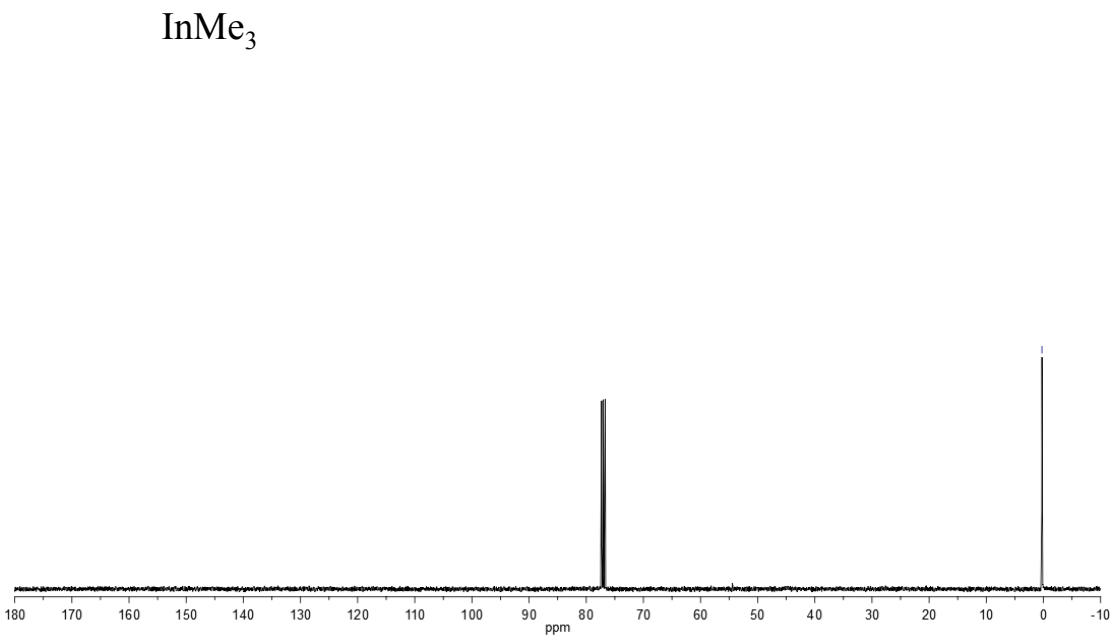

Figure S22. ^{1}H NMR (top) and ^{13}C (bottom) NMR spectra of **InMe$_3$** (∗ from residual $CHCl_3$ in $CDCl_3$).